DMD Fast Forward. Published on May 8, 2019 as DOI: 10.1124/dmd.119.086975
This article has not been copyedited and formatted. The final version may differ from this version.

DMD # 86975

Interactions of alectinib with human ABC drug efflux transporters and CYP biotransformation enzymes: effect on pharmacokinetic multidrug resistance

Jakub Hofman, Ales Sorf, Dimitrios Vagiannis, Simona Sucha, Eva Novotna, Sarah Kammerer, Jan-Heiner Küpper, Martina Ceckova, Frantisek Staud

Department of Pharmacology and Toxicology, Faculty of Pharmacy in Hradec Kralove, Charles University, Heyrovskeho 1203, 500 05 Hradec Kralove, Czech Republic (J.H., A.S., D.V., S.S., M.C., F.S.)

Department of Biochemical Sciences, Faculty of Pharmacy in Hradec Kralove, Charles University, Heyrovskeho 1203, 500 05 Hradec Kralove, Czech Republic (E.N.)

Institute of Biotechnology, Brandenburg University of Technology Cottbus-Senftenberg, Universitätsplatz 1, 01968, Senftenberg, Germany (S.K., J.-H. K.)

DMD Fast Forward. Published on May 8, 2019 as DOI: 10.1124/dmd.119.086975
This article has not been copyedited and formatted. The final version may differ from this version.

Running title: Alectinib inhibits ABCB1 and ABCG2 but not CYP enzymes

Corresponding author: RNDr. Jakub Hofman Ph.D., Department of Pharmacology and Toxicology, Faculty of Pharmacy in Hradec Kralove, Charles University, Akademika Heyrovskeho 1203, 500 05 Hradec Kralove, Czech Republic. Tel.: +420495067593, Fax: +420495067170, Email: jakub.hofman@faf.cuni.cz

Number of text pages: 38

Number of tables: 1

Number of figures: 9

Number of references: 49

Number of words in the *Abstract*: 218

Number of words in the *Introduction*: 750

Number of words in the *Discussion*: 1470

Abbreviations: ABC, ATP-binding cassette; ABCB1, P-glycoprotein; ABCC1, multidrug resistance-associated protein 1; ABCG2, breast cancer resistance protein; ALK, anaplastic lymphoma kinase; CI, combination index; C_{max}, maximum plasma concentration; CYP, cytochrome P450; DDI, drug-drug interaction; DMEM, Dulbecco's modified Eagle's medium; DMSO, dimethyl sulfoxide; EMA, European Medicines Agency; EMEM, Eagle's minimal essential medium; F_A, fraction of cells affected; FBS, fetal bovine serum; NBD, nucleotide-binding domain; US FDA, US Food and Drug Administration; IC_{50}, half-maximal inhibitory concentration; MDCKII, Madin-Darby canine kidney subtype 2 cell line; MDR, multidrug resistance; MTT, 3-(4,5-dimethyl-2-thiazolyl)-2,5-diphenyl-2H-tetrazolium bromide; NSCLC, non-small cell lung cancer; PBS, phosphate buffered saline; qRT-PCR, quantitative real-time reverse transcription PCR; RPMI-1640, Roswell Park Memorial Institute medium 1640; TKI, tyrosine kinase inhibitor

Abstract

Alectinib is a tyrosine kinase inhibitor currently used as a first-line treatment of ALK-positive metastatic non-small cell lung cancer (NSCLC). In the present work, we investigated possible interactions of this novel drug with ABC drug efflux transporters and cytochrome P450 (CYP) biotransformation enzymes that play significant roles in the phenomenon of multidrug resistance (MDR) of cancer cells as well as in pharmacokinetic drug-drug interactions. Using accumulation studies in MDCKII cells, alectinib was identified as an inhibitor of ABCB1 and ABCG2 but not of ABCC1. In subsequent drug combination studies, we demonstrated the ability for alectinib to effectively overcome MDR in ABCB1- and ABCG2-overexpressing MDCKII and A431 cells. To describe the pharmacokinetic interaction profile of alectinib in a complete fashion, its possible inhibitory properties toward clinically relevant CYP enzymes (i.e., CYP1A2, CYP2B6, CYP2C8, CYP2C9, CYP2C19, CYP2D6, CYP3A4 or CYP3A5) were evaluated using human CYP-expressing insect microsomes, revealing alectinib as a poor interactor. Advantageously for its use in pharmacotherapy, alectinib further exhibited negligible potential to cause any changes in expression of *ABCB1*, *ABCG2*, *ABCC1* and *CYP1A2*, *CYP3A4*, *CYP2B6* in intestine, liver and NSCLC models. Our *in vitro* observations might serve as a valuable foundation for future *in vivo* studies that could support the rational for our conclusions and possibly enable providing more efficient and safer therapy to many oncological patients.

DMD Fast Forward. Published on May 8, 2019 as DOI: 10.1124/dmd.119.086975
This article has not been copyedited and formatted. The final version may differ from this version.

Introduction

Globally, cancer is listed as the second major cause of death and is expected to surpass cardiovascular diseases in the next few years (Bhatnagar et al., 2015). Among cancerous diseases, lung cancer is far and away the leading killer and is responsible for approximately 25% of all cancer deaths in both men in women (Siegel et al., 2018). Clinical treatment of tumor diseases is today moving from classical cytotoxic agents to novel targeted drugs that are characterized by high efficacy and reduced toxicity (DeVita and Chu, 2008). Alectinib (Alecensa®) (Fig. 1) is a small molecule tyrosine kinase inhibitor (TKI) targeting fusion mutated anaplastic lymphoma kinase (ALK), which acts as an oncogenic driver in non-small cell lung cancer (NSCLC). This molecule gained accelerated approval by the US Food and Drug Administration (US FDA) in 2015 as a second-line treatment for patients with advanced ALK-positive NSCLC. Two years later, alectinib replaced crizotinib (Xalkori®) as the first-line treatment for ALK-positive metastatic NSCLC both in the USA and Europe (Muller et al., 2017), thus becoming an essential drug against this type of cancer.

ABC (ATP-binding cassette) drug efflux transporters comprise an important group of transmembrane proteins that are able to pump a variety of structurally unrelated xenobiotic compounds, including drugs, out of cells. These essential carriers are predominantly localized in organs with absorptive and eliminative functions (intestine, liver, kidney), as well as in body barriers (the brain, testes and placenta). According to their localizations, ABC drug efflux transporters act as body protection units limiting absorption and distribution while enhancing elimination of potentially harmful drugs. Such actions significantly affect the overall pharmacokinetic behavior of transporter substrates and create a rationale for clinically relevant pharmacokinetic drug-drug interactions (DDIs) (Szakacs et al., 2008). The superfamily of cytochromes P450 (CYPs) constitutes another crucial part of the body's detoxification capability and often cooperates with ABC drug efflux transporters in body

protection. These biotransformation enzymes metabolize a broad spectrum of drugs, thus enhancing their excretion. Similarly to ABC transporters, CYPs constitute an important site for pharmacokinetic DDIs (Wienkers and Heath, 2005). Investigation of novel chemical entities' interactions with ABC transporters and CYP enzymes is therefore strongly highlighted by drug regulatory authorities, who recommend also the use of *in vitro* methods for assessing interaction potential (Prueksaritanont et al., 2013). Although pharmacodynamic properties of alectinib have been studied extensively, only limited information is available regarding its pharmacokinetic behavior, and especially its interactions with ABC drug efflux transporters and CYP enzymes.

In addition to their beneficial protective functions in physiological tissues, some of the ABC drug efflux transporters and CYP metabolizing enzymes expressed in tumor cells have been reported to reduce the intracellular concentrations of the active forms of anticancer drugs below their cytotoxic levels. Among ABC transporters, ABCB1 (P-glycoprotein), ABCG2 (breast cancer resistance protein) and ABCC1 (multidrug resistance-associated protein 1) have been shown to participate in MDR *in vitro* and *in vivo* (Fletcher et al., 2010; Robey et al., 2018). In comparison with transporters, much less attention has been given to the role of metabolizing enzymes in MDR. Nevertheless, decreased efficacy of paclitaxel, docetaxel and vincristine has been clearly linked to the activities of CYP3A4/5 and CYP2C8 enzymes in tumors (Michael and Doherty, 2005; Rochat, 2009; Vadlapatla et al., 2013). Several attempts have been made to overcome ABC transporter-mediated resistance by co-administration of ABC transporter inhibitors with conventional cytotoxic drugs, but these compounds have failed in clinical trials due to insufficient efficacy and/or toxicity (Bugde et al., 2017). Apart from this strategy, targeting pharmacokinetic MDR mechanisms still has appealing potential. In particular, combining new-generation modulators identified among novel small molecule targeted drugs with conventional anticancer drugs has potential to become a new treatment

option for MDR cancers (Kathawala et al., 2015; Beretta et al., 2017). We have recently revealed inhibitory effects of several cyclin-dependent kinase inhibitors in relation to ABCB1, ABCG2 and/or ABCC1, as well as their abilities to reverse MDR of the ABC transporters-expressing cells toward conventional cytotoxic anticancer drugs (Hofman et al., 2012; Cihalova et al., 2013; Cihalova et al., 2015a; Cihalova et al., 2015b; Sorf et al., 2018). This dual mechanism could be proven advantageous and may imply a valuable role for these drugs in various chemotherapeutic regimens.

In the present work, we used a variety of *in vitro* techniques to investigate the potential for alectinib to become the perpetrator of DDIs mediated by ABC drug efflux transporters and/or CYPs. Furthermore, we tested the role of alectinib in pharmacokinetic MDR and its capability to overcome this unfavorable therapeutic obstacle.

Materials and methods

Reagents and chemicals

Alectinib was obtained from Selleckchem (Houston, TX, USA). Hoechst 33342 and calcein AM were from Sigma Aldrich (St. Louis, MO, USA) and Thermo Fisher Scientific (Waltham, MA, USA), respectively. Daunorubicin, mitoxantrone, dimethyl sulfoxide (DMSO), MTT, as well as cell culture reagents were purchased from Sigma Aldrich. Opti-MEM was supplied by Gibco BRL Life Technologies (Rockville, MD, USA). Hepatocyte Culture Medium and Hepatocyte High Performance Medium were from Upcyte Technologies (Hamburg, Germany). LY335979 (zosuquidar) was obtained from Toronto Research Chemicals (North York, ON, Canada), and Ko143 and MK-571 were from Enzo Life Sciences (Farmingdale, NY, USA). Insect cell microsomes containing recombinant human enzymes CYP1A2, CYP2B6, CYP2C8, CYP2C9, CYP2C19, CYP2D6, CYP3A4 or CYP3A5

were purchased as Vivid CYP450 Screening Kits from Thermo Fisher Scientific. CYP inhibitors α-naphthoflavone (CYP1A2), miconazole (CYP2B6 and CYP2C19), montelukast (CYP2C8), sulfaphenazole (CYP2C9), quinidine (CYP2D6) and ketoconazole (CYP3A4 and CYP3A5) were from Sigma Aldrich. Pierce BCA Protein Assay Kit was purchased from Thermo Fisher Scientific. TRI Reagent was purchased from Molecular Research Center (Cincinnati, OH, USA). TaqMan systems for the analyses of *ABCB1*, *ABCG2*, *ABCC1* and *CYP1A2*, *CYP3A4*, *CYP2B6* mRNA expressions, gb Reverse Transcription Kit and gb Easy PCR Master Mix were from Generi Biotech (Hradec Kralove, Czech Republic). All other chemicals and reagents were of the highest purity that was commercially available.

Cell cultures

Madin-Darby canine kidney (MDCKII) cell lines transduced for stable expression of human transporters ABCB1 (MDCKII-ABCB1), ABCG2 (MDCKII-ABCG2) or ABCC1 (MDCKII-ABCC1) and the control MDCKII-parent (MDCKII-par) cell line were all obtained from Dr. Alfred Schinkel (The Netherlands Cancer Institute, Amsterdam, The Netherlands). Human epidermoid carcinoma A431-parent cells and their ABCB1- and ABCG2-overexpressing variants A431-ABCB1 and A431-ABCG2, respectively, were kindly provided by Dr. Balasz Sarkadi (Hungarian Academy of Sciences, Budapest, Hungary) (Elkind et al., 2005). The MDCKII and A431 cells were grown in high-glucose DMEM supplemented with 10% fetal bovine serum (FBS). A549 (human NSCLC adenocarcinoma) cells were purchased from the American Type Culture Collection (Manassas, VA, USA) and were cultured under identical conditions as were the MDCKII sublines. Caco-2 (human colorectal adenocarcinoma) and NCI-H1299 (human NSCLC carcinoma) cell lines were purchased from the same source as A549 and were cultured in high-glucose DMEM supplemented with 10% FBS along with 1% nonessential amino acids and RPMI-1640 supplemented with 10% FBS, 1

mM sodium pyruvate and 10 mM HEPES, respectively. LS174T (human colorectal adenocarcinoma) cells were from the European Collection of Cell Cultures (Salisbury, UK) and were cultured in EMEM supplemented with 2 mM glutamine, 1% nonessential amino acids and 10% FBS. The unique model of proliferation-competent primary-like human hepatocytes HepaFH3 was kindly provided by Prof. Jan-Heiner Küpper (Brandenburgische Technische Universität, Cottbus-Senftenberg, Germany) (Herzog et al., 2016). These cells were cultured in complete Hepatocyte Culture Medium, and for experiments complete Hepatocyte High Performance Medium was used. Routine cultivations and all experiments were performed at standard conditions (37°C, 5% CO_2) in antibiotic-free medium. The cell lines were periodically tested for mycoplasma contamination. Cells from passages 10 to 25 were used in all experiments. DMSO was applied as a solvent for alectinib at concentrations that did not exceed 0.5%. No effects on the tested parameters were observed in the control experiments.

Cellular accumulation assay with hoechst 33342 and calcein AM

In brief, MDCKII-par, MDCKII-ABCB1, MDCKII-ABCG2 and MDCKII-ABCC1 were seeded at densities 5.0×10^4, 5.0×10^4, 5.5×10^4 and 6.0×10^4 cells/well on transparent 96-well plates 24 h before the experiment and incubated at 37°C in 5% CO_2 to grow to full confluence. Cells were then washed twice with 1 × PBS, Opti-MEM solutions of alectinib (0.1, 0.5, 1, 2.5 and 5 μM) and model specific inhibitors used as positive controls (1 μM LY335979, 1 μM Ko143 and 25 μM MK-571 for ABCB1, ABCG2 and ABCC1, respectively) were added, and plates were pre-incubated for 10 min at identical conditions. Hoechst 33342 (model substrate for ABCB1 and ABCG2) or calcein AM (model substrate for ABCC1) in Opti-MEM at final concentration of 8 or 2 μM, respectively, was added rapidly into all wells except blank samples and their intracellular levels were determined at 1 min

intervals for 30 min using an Infinite M200 Pro microplate reader (Tecan, Männedorf, Switzerland). Fluorescence was monitored in a bottom mode using excitation/emission wavelengths of 350/465 and 485/535 nm for hoechst 33342 and calcein AM, respectively.

Cellular accumulation assay with daunorubicin and mitoxantrone

MDCKII-par, MDCKII-ABCB1, MDCKII-ABCG2 and MDCKII-ABCC1 cells were seeded on a 12-well culture plate in a density of 1.5×10^5 cells/well and cultured for 24 h to reach 70–80% confluence. The cells were then washed once with 1 × PBS and treated with Opti-MEM solutions of alectinib (0.01, 0.1, 0.5, 1, 2.5 and 5 μM) or model specific inhibitors (1 μM LY335979, 1 μM Ko143 and 25 μM MK-571 for ABCB1, ABCG2 and ABCC1, respectively) and pre-incubated for 10 min at 37°C and 5% CO_2. Afterwards, daunorubicin (substrate for ABCB1 and ABCC1) or mitoxantrone (substrate for ABCG2) in Opti-MEM was added to the cells in the final concentration of 2 or 1 μM, respectively, with the exception of background samples. After 1 h incubation under the same conditions, the cells were put on ice, washed twice with ice cold 1 × PBS and lysed in lysis buffer (25 mM Tris, 150 mM NaCl, 1% Triton X-100) on an automatic shaker for 30 min at room temperature. The lysate was resuspended, harvested into Eppendorf tubes and subsequently centrifuged at 10 000 rpm for 5 min. Next, 100 μl of pure lysate free of cellular debris from each sample was transferred into black 96 well-plates and fluorescence was measured using an Infinite M200 Pro microplate reader (Tecan). The excitation/emission wavelengths for daunorubicin and mitoxantrone were 490/565 and 640/670 nm, respectively. The protein contents of cell lysates were assessed via bicinchoninic acid method employing a Pierce BCA Protein Assay Kit. RFU values obtained in fluorescence measurements were normalized to protein content.

Molecular docking simulations

Alectinib was downloaded from the Zinc Database (http://zinc.docking.org) (Irwin et al., 2012) and its energy was minimized using CSChemOffice version 18.0 (Cambridge Soft, Cambridge, MA, USA). The structures of ABCB1 were obtained from the Protein Data Bank (http://www.rcsb.org; PDB ID 4M2S and 6C0V) (Li et al., 2014; Kim and Chen, 2018). A homology model of the inward-facing form was generated using the crystal structure of mouse Abcb1 (PDB ID 4M2S) (Li et al., 2014) and primary sequence of human ABCB1 (P08183) (UniProt, 2019) by means of Swiss-Model Workspace accessible via the ExPaSy web server (Guex et al., 2009; Bienert et al., 2017; Waterhouse et al., 2018). In the case of the outward-facing form, Swiss-Model Workspace was employed to generate a homology model with Gln-556 and Gln-1201 mutated to catalytically active Glu using the same human ABCB1 sequence and 6C0V as a template. Both alectinib and ABCB1 were further prepared for docking using MGL Tools 1.5.6 (Morris et al., 2009). In the case of the protein, all water molecules, ATP and ligands were removed; hydrogens and Gasteiger charges were then added. Docking calculations were carried out with AutoDock Vina 1.1.2 (Trott and Olson, 2010). Rigid docking was performed using an 80 × 80 × 80 grid box positioned into the internal cavity of the inward-facing form (x = 18.62, y = 55.05, z = −0.82). Flexible docking was further performed into both inward- and outward-facing forms of ABCB1. Docking into the M-site of the inward-facing form involves nine flexible protein residues (Phe-303, Tyr-307, Ile-340, Phe-343, Gln-347, Gln-725, Phe-728, Phe-983 and Gln-990), and the size of the grid box was decreased to 20 × 20 × 20. In the case of R-site docking, five residues (Thr-240, Asp-241, Leu-244, Lys-826 and Phe-994) were assigned as flexible and a 40 × 40 × 40 grid box was placed into the R-site position (x = 9.83, y = 83.03, z = 17.98). The flexible part of the outward-facing form of ABCB1 contains nine residues (Asp-164, Tyr-401, Arg-404, Ile-409, Lys-433, Thr-435, Gln-475, Gln-1175 and Gln-1180) for docking into nucleotide-

binding domain 1 (NBD1) and seven residues (Gln-530, Tyr-1044, Arg-1047, Val-1052, Lys-1076, His-1232 and Gln-1118) for docking into NBD2. The 40 × 40 × 40 grid box was positioned into ATP-binding sites (x = 172.27, y = 190.31, z = 132.08 and x = 156.69, y = 168.89, z = 119.33). The exhaustiveness parameter was set to 8 for all docking calculations. PyMOL 1.8.6.0 (The PyMOL Molecular Graphics System, Schrödinger, LLC) was employed to visualize the interactions.

The structures of ABCG2 downloaded from the Protein Data Bank (PDB ID 6HIJ and 6HBU) (Jackson et al., 2018; Manolaridis et al., 2018) were prepared for docking using MGL Tools 1.5.6 as described for ABCB1. Because the crystal structure with PDB ID 6HBU had been deposited into Protein Data Bank with mutation E211Q, Swiss-Model Workspace was used to change Gln-211 in NBDs back to Glu-211 utilizing the primary sequence of human ABCG2 (Q9UNQ0) (UniProt, 2019) and crystal structure 6HBU as a template. AutoDock Vina was further employed for docking using the same conditions (size of grid boxes and exhaustiveness) as described above. Docking calculations were carried out into ligand-binding internal cavity (x = 129.81, y = 129.91, z = 142.89, PDB ID 6HIJ) and NBDs (x = 113.32, y = 92.03, z = 129.89 and x = 94.09, y = 115.37, z = 129.96, PDB ID 6HBU). Six residues were assigned as flexible (Phe-432, Phe-439, Leu-539, Ile-543, Val-546, Met-549) in cases of flexible docking analysis performed into the internal cavity.

Inhibitory assay for human recombinant CYPs

CYP3A4, CYP3A5 and CYP2C8, enzymes participating in cytostatic drug resistance, as well as all other CYP enzymes recommended to be tested for inhibition by US FDA and the European Medicines Agency (EMA) (i.e., CYP1A2, CYP2B6, CYP2C9, CYP2C19 and CYP2D6), were included in the evaluation. Inhibition was tested employing Vivid CYP450 Screening Kits that contain microsomal preparations from insect cells expressing particular

recombinant human CYP enzymes. Experiments were performed according to the manufacturer's instructions in a kinetic mode. Time-dependent generation of fluorescent metabolite was recorded at 1 min intervals for 60 min using an Infinite M200 Pro microplate reader (Tecan). The enzyme concentration and incubation interval used for data evaluation (15 min) were within the linear part of the appropriate reaction velocity curves. Final concentration of DMSO used as an alectinib solvent did not exceed 0.5%, and activity changes caused by DMSO were corrected using appropriate controls. Model inhibitors recommended by the manufacturer were utilized as positive controls in all experiments.

MTT proliferation assay

Cells were seeded at the following densities (cells/well): 1.3×10^4 for MDCKII-par, MDCKII-ABCB1, MDCKII-ABCG2 and MDCKII-ABCC1; 1.2×10^4 for A431-parent and A431-ABCB1; 1.0×10^4 for A431-ABCG2; 0.80×10^4 for A549; 0.75×10^4 for NCI-H1299; 2.0×10^4 for Caco-2; 5.0×10^4 for LS174T; and 1.0×10^4 for HepaFH3 on 96-well culture plates and cultured for 24 h to reach 50% confluence. The medium was then replaced with fresh medium containing the tested drugs or drug combinations. Cell viability was determined after 48 h of incubation under standard conditions (37°C, 5% CO_2). The medium was aspirated and cells were washed once with prewarmed 1 × PBS. MTT solution in Opti-MEM (1 mg/ml) was added to the cells, and cells were subsequently incubated at standard conditions for 60 (MDCKII-cell lines and HepaFH3 cells) or 45 min (all other cell lines). The solution was aspirated and the cells were lysed with DMSO on an automatic shaker for 10 min. Absorbance was measured at 570 nm and 690 nm using an Infinite M200 Pro microplate reader (Tecan). The background values of 690 nm were subtracted from those values obtained at 570 nm. For the normalization of absorbance values, absorbance from cells where only medium had been added was considered as 100% viability. Absorbance equal to 0% viability

was obtained from cells incubated in 10% DMSO. The method was used to 1) assess the effect of ABCB1, ABCG2 or ABCC1 on sensitivity of MDCKII cells to alectinib, 2) assess alectinib's potential to reverse MDR in drug combination assays, and 3) estimate the concentrations to be used in induction studies.

Drug combination assays

MDCKII and A431 sublines were seeded (see densities above) on 96-well culture plates and cultured for 24 h to reach 50% confluence. The medium was then replaced with fresh medium containing concentration ranges of alectinib alone or of a model cytostatic (daunorubicin or mitoxantrone) with or without 2 μM (daunorubicin combinations) or 1 μM (mitoxantrone combinations) alectinib. Cell viability was determined after 48 h of incubation at standard conditions (37°C, 5% CO_2) according to the procedure described above. Obtained data were converted to F_A (fraction of cells affected) data and the drug combination effect was quantified according to the combination index (CI) method of Chou-Talalay using CompuSyn 3.0.1 software (ComboSyn Inc., Paramus, NJ, USA). Based on the CI values, the effects of simultaneously administered drugs were marked as either synergistic ($CI < 0.9$), additive ($CI = 0.9 – 1.1$) or antagonistic ($CI > 1.1$) (Chou, 2006).

Gene induction studies

First, a suitable concentration of alectinib for gene expression studies was chosen using the MTT proliferation method (see above). For gene induction studies, A549 (24×10^4 cells/well), NCI-H1299 (18×10^4 cells/well), Caco-2 (50×10^4 cells/well), LS174T (100×10^4 cells/well) or HepaFH3 (40×10^4 cells/well) cells were seeded on 12-well plates 24 h before the experiment. At time 0, the medium was replaced with fresh medium containing 0.5

μM alectinib or fresh medium containing 0.005% DMSO (vehicle control). Samples were taken at 24 and 48 h intervals. Total RNA from the cells was isolated using TRI Reagent and chloroform according to the manufacturer's instructions. After isolation, the RNA quality and integrity were verified by agarose gel electrophoresis. DNase treatment was not performed prior to reverse transcription because all TaqMan quantitative real-time reverse transcription PCR (qRT-PCR) systems were designed to span introns and/or cross intron/exon boundaries. Reverse transcription was conducted using a commercial gb Reverse Transcription Kit, and 1000 ng of RNA was transcribed into the corresponding cDNA in one reaction. *ABCB1*, *ABCG2*, *ABCC1* and *CYP1A2*, *CYP3A4*, *CYP2B6* mRNA levels were determined using a commercial gb Easy PCR Master Mix and a TaqMan qRT-PCR systems in 384-well plates according to the manufacturer's instructions while amplifying 20 ng of cDNA per reaction. Relative quantification of the examined ABC transporters and CYP enzymes was performed using the ΔΔCt method; the geometric mean of *B2M* and *HPRT1* levels was used as an internal control to normalize the variability in expression levels. qRT-PCR analysis was performed on a QuantStudio 6 apparatus (Life Technologies, Carlsbad, CA, USA) with initial denaturation at 95°C for 3 min and 40 repeats of a cycle consisting of 95°C for 10 s and 60°C for 20 s.

Statistical analysis

Statistical analysis was performed using GraphPad Prism software version 7.03 (GraphPad Software Inc., La Jolla, CA, USA). The *p* values were calculated using one-way ANOVA followed by Dunnett's post hoc test or a two-tailed unpaired *t*-test. Differences of $p < 0.05$ were considered statistically significant. GraphPad Prism software was also used to calculate the half-maximal inhibitory concentrations (IC_{50}) while applying nonlinear regression analysis using sigmoidal Hill kinetics (ABC transporter- and CYP-inhibitory

assays, proliferation experiments) and to normalize the raw data (CYP inhibitory assays and proliferation experiments). All experiments were performed as three independent repetitions with biological triplicates in each repetition.

Results

Effect of alectinib on intracellular accumulation of hoechst 33342 or calcein AM in MDCKII sublines

First, alectinib's ability to inhibit ABC transporter-mediated efflux of hoechst 33342 or calcein AM was investigated in MDCKII sublines. Alectinib significantly increased hoechst 33342 accumulation in both MDCKII-ABCB1 and MDCKII-ABCG2 cells, reaching inhibitory potency of model inhibitor only in MDCKII-ABCG2 cells. Data analysis revealed relative IC_{50} values of 0.399 μM and >5.00 μM for ABCG2 and ABCB1 transporter inhibition, respectively. In contrast, no inhibitory effect of alectinib on ABCC1-mediated efflux of calcein AM was observed (Fig. 2).

Influence of alectinib on intracellular accumulation of daunorubicin or mitoxantrone in MDCKII sublines

To confirm results obtained in experiments with hoechst 33342 and calcein AM, we subsequently performed transporter inhibitory studies using daunorubicin (ABCB1, ABCC1 substrate) and mitoxantrone (ABCG2 substrate). At the same time, these second-line accumulation experiments clarified alectinib to be applicable as an MDR modulator inasmuch as the same drugs were further employed as model agents in follow-up drug combination studies.

As in the previous case, alectinib significantly increased accumulation of model substrates in both MDCKII-ABCB1 and MDCKII-ABCG2 cells, yielding IC_{50} values of 1.27

and 0.453 μM, respectively. Similar to the results of the calcein AM assay, alectinib did not affect daunorubicin accumulation in MDCKII-ABCC1 cells even at the highest concentration tested (Fig. 3).

Molecular docking of alectinib into ABCB1 and ABCG2

To investigate the observed alectinib interaction with ABCB1 and ABCG2 at molecular level, *in silico* docking simulations were performed. Rigid molecular docking into the inward-facing form of ABCB1 predicted two potential binding sites for alectinib: one close to the apex of the internal V-shaped cavity (-10.2 to -8.9 kcal/mol) and another at a lower location (-8.7 kcal/mol), described previously as modulator site (M-site) and rhodamine-binding site (R-site), respectively (Ferreira et al., 2013). In contrast, no interaction was observed on a third ligand-binding site specific for hoechst 33342 (H-site) (Fig. 4A). To mimic real conditions regarding possible ABCB1 conformations, the residues in the M- and R-sites predicted to interact with alectinib were set as flexible and molecular docking was repeated. The flexible docking analysis has shown that alectinib probably interacts with Met-69, Phe-303, Tyr-307, Phe-336, Ile-340, Phe-343, Gln-725, Phe-728, Phe-732, Phe-983, Met-986, Gln-990, and Phe-994 (-12.5 kcal/mol) at the M-site and with Phe-770, Gln-773, Glu-782, Ala-823, Lys-826, Phe-994 and Pro-996 at the R-site (-9.4 kcal/mol) of ABCB1 (Fig. 4B). Because alectinib is an ATP-competitive inhibitor of its target ALK kinase (Song et al., 2015), we considered its potential interaction with NBDs of ABCB1 and docked alectinib at the ATP-binding site. The results of flexible molecular modeling show that alectinib may additionally compete with ATP (-12.3 and -12.1 kcal/mol) and thereby indirectly inhibit ABCB1 efflux function (Fig. 4C).

In contrast to ABCB1, ABCG2 is a homodimer that contains two cavities (internal and external) separated by Leu-554 of opposing monomers. However, only the internal cavity can

bind ligands (Jackson et al., 2018). In our experiments, both rigid and flexible molecular docking positioned alectinib in the internal cavity, thereby showing that two molecules are necessary to lock ABCG2 into an inward-facing conformation (Fig. 4D). Further docking into NBDs of ABCG2 predicted that alectinib may probably compete with ATP for binding to NBDs (-8.8 and -8.6 kcal/mol) (Fig. 4E), albeit with significantly lower affinity than that predicted for the internal ligand binding cavity (-13.1 and -13.0 kcal/mol).

Modulatory effects of alectinib on ABC transporter-mediated cytostatic MDR

In the follow-up experiments, we investigated whether inhibitory interactions of alectinib with ABC efflux transporters could be utilized for overcoming resistance to the recognized ABCB1 and ABCG2 substrates daunorubicin and mitoxantrone, respectively. These studies were first performed in MDCKII sublines, and the results were then confirmed in a physiologically more relevant model of human cytostatic resistant A431 sublines (Elkind et al., 2005). The modulatory concentrations of alectinib (2 or 1 μM for daunorubicin or mitoxantrone combinations, respectively) in experiments were carefully selected to fit the following criteria: (1) causing sufficient inhibition of ABC transporter, (2) being only negligibly cytotoxic to model cell lines, and (3) being clinically relevant based on C_{max} recorded in *in vivo* pharmacokinetic studies in patients.

Alectinib was shown to effectively overcome daunorubicin and mitoxantrone resistance in ABC transporter-overexpressing cells, yielding fold reversal values of 17.8 and 9.64 in MDCKII-ABCB1 and MDCKII-ABCG2 cells, respectively. The tested TKI was similarly active in A431 cells, reaching fold reversal values of 24.4 and 44.3 for ABCB1 and ABCG2 overexpressing variant sublines, respectively. Although 1 or 2 μM alectinib concentration caused only 7 or 11% and 6 or 24% viability decrease in MDCKII-par and A431-par cells, respectively, we observed unexpected sensitization of these control cells to

daunorubicin's and mitoxantrone's effects. To subtract the non-transporter mediated sensitization effect, we normalized fold reversal data from transporter-overexpressing cells to the fold reversal data from parent cells. Obtained normalized fold reversal values of 6.18, 6.79, 2.14 and 4.81 in MDCKII-ABCB1, MDCKII-ABCG2, A431-ABCB1 and A431-ABCG2 cells, respectively, clearly reflect the participation of alectinib-caused ABCB1 and ABCG2 inhibitory effect in overcoming daunorubicin and mitoxantrone resistance (Fig. 5, Table 1). The involvement of inhibition of ABC efflux pumps in this process was further confirmed by employing data analysis according to the combination index method of Chou-Talalay, a method in wide use and that offers quantitative definition for additive effect, synergism or antagonism in drug combination studies. In addition to antagonistic and additive effects, synergism was also recorded in parent cells at higher F_A range, but its extent was considerably lower in comparison with ABC transporter-overexpressing cells (Fig. 6).

Effect of ABCB1, ABCG2 and ABCC1 overexpression on cell resistance to alectinib

In addition to evaluating MDR-modulatory properties of alectinib, we also investigated whether ABC transporters could be the potential causative mechanism for developing cellular resistance to this TKI similar to standard cytostatics. The results of MTT proliferation studies showed no significant changes in alectinib antiproliferative effect between MDCKII-par and ABC transporter-transduced MDCKII sublines (Fig. 7), thus suggesting an improbable role for ABCB1-, ABCG2- or ABCC1-efflux activity in the establishment of MDR to alectinib.

Alectinib does not affect activity of clinically relevant CYP enzymes

To evaluate whether alectinib might bear a potential to affect enzyme-mediated pharmacokinetic resistance to paclitaxel, docetaxel, or vincristine, and to become a perpetrator of DDIs, *in vitro* inhibitory assays with human recombinant CYP3A4, CYP3A5

and CYP2C8 were performed. The testing was further broadened to include other clinically relevant enzymes playing predominant roles in pharmacokinetic DDIs (i.e., CYP1A2, CYP2B6, CYP2C9, CYP2C19 and CYP2D6). Alectinib was demonstrated to be a poor interactor, since it did not reach an inhibitory level greater than 20% in any of these eight CYP enzymes even at the highest concentration tested (Fig. 8).

Changes in ABCB1, ABCG2, ABCC1 and CYP1A2, CYP3A4, CYP2B6 expressions following exposure to alectinib

Apart from inhibition, the induction of ABC transporters and CYPs by alectinib could constitute another phenomenon that is able to affect the pharmacological fate of concomitantly administered drugs. To address this possibility, we performed gene expression studies focused on *ABCB1, ABCG2, ABCC1* and *CYP1A2*, *CYP3A4, CYP2B6* in suitable intestine (LS174T, Caco-2) and hepatic (HepaFH3) cellular models, respectively. In addition, possible changes in *ABCB1*, *ABCG2,* and *ABCC1* gene expressions following exposure to alectinib were assessed in NSCLC cellular models (A549 and NCI-H1299) to reveal whether this TKI could affect MDR phenotype of its target cancer cells.

The concentration of alectinib (0.5 μM) in the experiments was carefully selected to fit the following criteria: (1) being only negligibly cytotoxic to model cell lines (Fig. 9A), and (2) being clinically relevant based on C_{max} recorded in *in vivo* pharmacokinetic studies in patients. Alectinib did not increase or decrease mRNA levels of the investigated ABC transporters and CYPs by more than 100% or 50% in any of the cases (Fig. 9B–F). In accordance with EMA guidelines (EMA, 2012), therefore, the results obtained cannot be considered positive for induction or down-regulation. That means alectinib's potential to become a perpetrator of induction-based DDIs as well as to influence MDR phenotype of its target cancer cells is low.

Discussion

Alectinib has become an essential drug for the treatment of patients suffering from fusion ALK-mutated forms of metastatic NSCLC (Muller et al., 2017). Although pharmacodynamic properties of this drug have been well understood, its pharmacokinetic interactions with transport proteins and biotransformation enzymes remain to be elucidated. In the present work, we investigated alectinib interactions with selected ABC drug efflux transporters and CYP enzymes and evaluated their possible utilization for overcoming pharmacokinetic MDR.

First, we investigated possible inhibition of ABCB1, ABCG2 and ABCC1 by alectinib in MDCKII sublines. While we obtained almost identical inhibitory characteristics toward ABCG2 and ABCC1 for both hoechst 33342/calcein AM and daunorubicin/mitoxantrone, the extent of ABCB1 inhibition varied considerably between model substrates. Molecular docking revealed that alectinib binds to M-site and R-site (specific for daunorubicin), but not to H-site (specific for hoechst 33342), thus explaining this discrepancy. It is noteworthy that our results highlight preferential affinity of substrates and inhibitors for any of the three ABCB1 binding sites as an important factor to consider when investigating and predicting ABCB1-mediated drug-drug interactions. Both interaction with substrate-binding sites and competition with ATP observed in our docking studies are in accordance with recent reports as to the competitive nature of ABCB1 inhibition by alectinib (Yang et al., 2017). Importantly, ABCB1 as well as ABCG2 inhibitory activity of alectinib might be clinically relevant and worthy of further evaluations including *in vivo* studies inasmuch as the steady-state C_{max} after maximum dose administration [I] divided by the IC_{50} as we assessed *in vitro* was substantially >0.1 (International Transporter Consortium et al., 2010). The alectinib steady-state C_{max} assessed in clinical trials evaluating standard dosing of 600 mg twice daily was equal to 1.38 μM (Zhu and Ou, 2017).

Having confirmed ABCB1 and ABCG2 inhibition by alectinib, we hypothesized that these interactions could be favorably exploited for the modulation of MDR to cytostatic drugs, such as daunorubicin or mitoxantrone. To test this hypothesis, we combined these conventional anticancer drugs with alectinib in ABC transporter-overexpressing vs. parental MDCKII and A431 cells and observed effective enhancement of their cytostatic effects in both cellular models. This is in accordance with recent description of alectinib's ability to potentiate the anticancer effect of such various cytostatic drugs as paclitaxel or doxorubicin in several ABC transporter-overexpressing cell lines, leukemic xenografts and primary leukemic cells (Yang et al., 2017). In addition to simple demonstration of the potential for alectinib to reverse MDR, we also focused in our studies on exact quantification of combination effects. In ABC transporter-overexpressing cells, synergism was detected as the outcome for the examined combinations across almost the whole range of F_A. This is an important finding, because synergistic combinations are frequently used in oncological clinical practice and allow for reducing the doses of drugs concomitantly used while dramatically increasing the safety and/or efficacy of a treatment (Bayat Mokhtari et al., 2017). Based on our results, it is possible to presume that synergism observed between alectinib and ABC transporter cytotoxic substrates could allow for considerable dose reduction that, in turn, would help to avoid occurrence of such severe side effects as bradycardia; muscle, liver, lung or kidney damage; myelosuppression; gastrointestinal or reproductive toxicity, and secondary carcinogenesis. In parental cell sublines, we also observed synergism between the examined drugs in certain parts of the F_A range. Its level was nevertheless substantially less than seen in transporter-overexpressing cells. These results suggest that although ABC transporter inhibitory effects play the decisive role in the recorded MDR modulatory capabilities of alectinib, there presumably exists some additional pharmacodynamic and/or pharmacokinetic mechanism contributing to the overall beneficial outcome of the tested drug combinations. Only limited

information is available about synergistic combinations of alectinib with other anticancer drugs, but experimental data suggest MET or mTOR pathways to be the molecular targets to be hit concomitantly with alectinib-inhibited ALK pathway in order to produce such effect (Kogita et al., 2015; Redaelli et al., 2016). Similarly, in the clinical area, alectinib has not yet been approved in any combination for cancer therapy, and only three drug combinations are currently waiting to be evaluated in early clinical trials, namely those including atezolizumab, cobimetinib and bevacizumab (ClinicalTrials.gov Identifiers NCT02013219, NCT03202940 and NCT02521051, respectively).

Apart from evaluating alectinib as a possible effective modulator, we aimed to look at the possible broadly opposite role of alectinib in pharmacokinetic MDR, which is to say whether its therapeutic effect could be compromised by this phenomenon. The results of MTT proliferation studies showed no significant changes in alectinib's antiproliferative effect between MDCKII-par and ABC transporter-transduced MDCKII sublines, thus suggesting lack of impact on tumor response to alectinib from the presence of MDR-causing ABC transporters. These data correlate well with those reported by Kodama et al., who designated alectinib as an ABCB1 non-substrate using *in vitro* Caco-2 bidirectional transport assays and hypothesized that this fact constitutes a background principle for efficient penetration of alectinib into the brain (Kodama et al., 2014). Later, an absence of ABCB1 substrate properties of alectinib was indirectly confirmed in a study showing that ABCB1 overexpression is able to confer resistance to ceritinib but not to alectinib (Katayama et al., 2016). In contrast, no detailed published information is available regarding alectinib substrate affinity to either ABCG2 or ABCC1 or their roles in the development of resistance toward alectinib. In light of our results, alectinib shows ideal characteristics as an MDR reversal agent whose modulatory properties are not compromised due to efflux by any of the MDR-associated transporters. This limitation in being both a high-affinity transporter inhibitor and

substrate is rather often seen for other TKIs acting as dual-mechanism drugs (Deng et al., 2014).

Along with ABC transporters, biotransformation enzymes represent additional causative factors participating in the development of pharmacokinetic MDR. To describe the possible role of alectinib in enzyme-meditated MDR, we further evaluated its interactions with CYP3A4, CYP3A5 and CYP2C8, which have been linked to decreased efficacy of paclitaxel, docetaxel and vincristine in tumors. At the same time, these enzymes play predominant roles in pharmacokinetic drug-drug interactions together with CYP1A2, CYP2B6, CYP2C9, CYP2C19 and CYP2D6. To cover also this issue, we included into our study all these eight CYPs that have been recommended by US FDA and EMA to be tested for inhibition (EMA, 2012; FDA, 2017). Alectinib inhibited none of the enzymes tested at clinically relevant concentrations and thus lacks the potential for modulation of enzyme-mediated MDR as well as for acting as a perpetrator of clinically relevant DDIs. It has previously been reported that alectinib is mainly metabolized by cytochrome CYP3A to a major, similarly active metabolite, M4 (Morcos et al., 2017; Nakagawa et al., 2018). In addition, alectinib has been described as a weak inhibitor of CYP3A, but alectinib has not been confirmed as either a victim or perpetrator by three *in vivo* drug-drug interaction studies involving healthy subjects and cancer patients (Morcos et al., 2017).

Apart from the inhibition, the induction of ABC transporters and CYPs by alectinib could constitute another phenomenon that is able to affect the pharmacological fate of concomitantly administered drugs. To address this possibility, we performed gene expression studies focused on *ABCB1, ABCG2, ABCC1* and *CYP1A2, CYP3A4, CYP2B6* in suitable intestine (LS174T, Caco-2) and hepatic (HepaFH3) models, respectively. In addition, possible changes in *ABCB1, ABCG2* and *ABCC1* gene expressions following exposure to alectinib were assessed in NSCLC cellular models (A549 and NCI-H1299) to reveal whether this TKI

could affect the MDR phenotype of its target cancer cells. Alectinib did not provoke gene expression changes that would fit the criteria given by EMA for induction or down-regulation (EMA, 2012), and therefore its potential to become a perpetrator of induction-based DDIs as well as to influence MDR phenotype of its target cancer cells can be considered low. No published information is available about induction potential of alectinib in relation to ABC drug efflux transporters. Regarding CYPs, it was recently reported that alectinib is able to weakly induce CYP3A4 *in vitro* but that this phenomenon does not translate into any clinically meaningful effects, as observed by an *in vivo* DDI study with midazolam (Morcos et al., 2017).

In summary, we provide clear evidence that alectinib is an inhibitor of ABCB1 and ABCG2 but not of ABCC1 transporter, and that it is able to effectively modulate transporter-mediated pharmacokinetic cytostatic resistance in a synergistic manner at clinically relevant concentrations. Importantly, alectinib shows ideal characteristics as an MDR reversal agent whose modulatory properties are not compromised due to efflux by any MDR-associated transporters. Furthermore, this TKI drug shows negligible potential to cause changes in the activities of CYP enzymes as well as in the gene expression levels of the examined CYPs and ABC transporters. Our *in vitro* observations might serve as a valuable basis for future *in vivo* studies that could support the rational for our conclusions and possibly enable providing more efficient and safer therapy to many oncological patients.

Authorship Contributions

Participated in research design: Hofman, Ceckova, and Staud.

Conducted experiments: Hofman, Sorf, Vagiannis, Sucha, and Novotna.

Contributed new reagents or analytic tools: Kammerer and Küpper.

Performed data analysis: Hofman, Sorf, Vagiannis, Sucha, and Novotna.

Wrote or contributed to the writing of the manuscript: Hofman, Sorf, Vagiannis, Sucha, Novotna, Kammerer, Küpper, Ceckova, and Staud.

References

Bayat Mokhtari R, Homayouni TS, Baluch N, Morgatskaya E, Kumar S, Das B, and Yeger H (2017) Combination therapy in combating cancer. *Oncotarget* **8:**38022-38043.

Beretta GL, Cassinelli G, Pennati M, Zuco V, and Gatti L (2017) Overcoming ABC transporter-mediated multidrug resistance: The dual role of tyrosine kinase inhibitors as multitargeting agents. *Eur J Med Chem* **142:**271-289.

Bhatnagar P, Wickramasinghe K, Williams J, Rayner M, and Townsend N (2015) The epidemiology of cardiovascular disease in the UK 2014. *Heart* **101:**1182-1189.

Bienert S, Waterhouse A, de Beer TAP, Tauriello G, Studer G, Bordoli L, and Schwede T (2017) The SWISS-MODEL Repository-new features and functionality. *Nucleic Acids Res* **45:**D313-D319.

Bugde P, Biswas R, Merien F, Lu J, Liu DX, Chen M, Zhou S, and Li Y (2017) The therapeutic potential of targeting ABC transporters to combat multi-drug resistance. *Expert Opin Ther Targets* **21:**511-530.

Cihalova D, Ceckova M, Kucera R, Klimes J, and Staud F (2015a) Dinaciclib, a cyclin-dependent kinase inhibitor, is a substrate of human ABCB1 and ABCG2 and an inhibitor of human ABCC1 in vitro. *Biochem Pharmacol* **98:**465-472.

Cihalova D, Hofman J, Ceckova M, and Staud F (2013) Purvalanol A, olomoucine II and roscovitine inhibit ABCB1 transporter and synergistically potentiate cytotoxic effects of daunorubicin in vitro. *PLoS One* **8:**e83467.

Cihalova D, Staud F, and Ceckova M (2015b) Interactions of cyclin-dependent kinase inhibitors AT-7519, flavopiridol and SNS-032 with ABCB1, ABCG2 and ABCC1 transporters and their potential to overcome multidrug resistance in vitro. *Cancer Chemother Pharmacol* **76:**105-116.

Deng J, Shao J, Markowitz JS, and An G (2014) ABC transporters in multi-drug resistance and ADME-Tox of small molecule tyrosine kinase inhibitors. *Pharm Res* **31:**2237-2255.

DeVita VT, Jr. and Chu E (2008) A history of cancer chemotherapy. *Cancer Res* **68:**8643-8653.

Elkind NB, Szentpetery Z, Apati A, Ozvegy-Laczka C, Varady G, Ujhelly O, Szabo K, Homolya L, Varadi A, Buday L, Keri G, Nemet K, and Sarkadi B (2005) Multidrug transporter ABCG2 prevents tumor cell death induced by the epidermal growth factor receptor inhibitor Iressa (ZD1839, Gefitinib). *Cancer Res* **65:**1770-1777.

EMA (2012) Guideline on the investigation of drug interactions. 21 June 2012 CPMP/EWP/560/95/Rev. 1 Corr. 2**.

FDA (2017) In Vitro Metabolism- and Transporter- Mediated Drug-Drug Interaction Studies Guidance for Industry. October 2017, Clinical Pharmacology, Silver Spring.

Ferreira RJ, Ferreira MJ, and dos Santos DJ (2013) Molecular docking characterizes substrate-binding sites and efflux modulation mechanisms within P-glycoprotein. *J Chem Inf Model* **53:**1747-1760.

Fletcher JI, Haber M, Henderson MJ, and Norris MD (2010) ABC transporters in cancer: more than just drug efflux pumps. *Nat Rev Cancer* **10:**147-156.

Guex N, Peitsch MC, and Schwede T (2009) Automated comparative protein structure modeling with SWISS-MODEL and Swiss-PdbViewer: A historical perspective. *Electrophoresis* **30:**S162-S173.

Herzog N, Hansen M, Miethbauer S, Schmidtke KU, Anderer U, Lupp A, Sperling S, Seehofer D, Damm G, Scheibner K, and Kupper JH (2016) Primary-like human hepatocytes genetically engineered to obtain proliferation competence display hepatic differentiation characteristics in monolayer and organotypical spheroid cultures. *Cell Biol Int* **40:**341-353.

Hofman J, Ahmadimoghaddam D, Hahnova L, Pavek P, Ceckova M, and Staud F (2012) Olomoucine II and purvalanol A inhibit ABCG2 transporter in vitro and in situ and synergistically potentiate cytostatic effect of mitoxantrone. *Pharmacol Res* **65:**312-319.

Chou TC (2006) Theoretical basis, experimental design, and computerized simulation of synergism and antagonism in drug combination studies. *Pharmacol Rev* **58:**621-681.

International Transporter Consortium, Giacomini KM, Huang SM, Tweedie DJ, Benet LZ, Brouwer KL, Chu X, Dahlin A, Evers R, Fischer V, Hillgren KM, Hoffmaster KA, Ishikawa T, Keppler D, Kim RB, Lee CA, Niemi M, Polli JW, Sugiyama Y, Swaan PW, Ware JA, Wright SH, Yee SW, Zamek-Gliszczynski MJ, and Zhang L (2010) Membrane transporters in drug development. *Nat Rev Drug Discov* **9:**215-236.

Irwin JJ, Sterling T, Mysinger MM, Bolstad ES, and Coleman RG (2012) ZINC: a free tool to discover chemistry for biology. *J Chem Inf Model* **52:**1757-1768.

Jackson SM, Manolaridis I, Kowal J, Zechner M, Taylor NMI, Bause M, Bauer S, Bartholomaeus R, Bernhardt G, Koenig B, Buschauer A, Stahlberg H, Altmann KH, and Locher KP (2018) Structural basis of small-molecule inhibition of human multidrug transporter ABCG2. *Nat Struct Mol Biol* **25:**333-340.

Katayama R, Sakashita T, Yanagitani N, Ninomiya H, Horiike A, Friboulet L, Gainor JF, Motoi N, Dobashi A, Sakata S, Tambo Y, Kitazono S, Sato S, Koike S, John Iafrate A, Mino-Kenudson M, Ishikawa Y, Shaw AT, Engelman JA, Takeuchi K, Nishio M, and Fujita N (2016) P-glycoprotein Mediates Ceritinib Resistance in Anaplastic Lymphoma Kinase-rearranged Non-small Cell Lung Cancer. *EBioMedicine* **3:**54-66.

Kathawala RJ, Gupta P, Ashby CR, Jr., and Chen ZS (2015) The modulation of ABC transporter-mediated multidrug resistance in cancer: a review of the past decade. *Drug Resist Updat* **18:**1-17.

Kim Y and Chen J (2018) Molecular structure of human P-glycoprotein in the ATP-bound, outward-facing conformation. *Science* **359:**915-919.

Kodama T, Hasegawa M, Takanashi K, Sakurai Y, Kondoh O, and Sakamoto H (2014) Antitumor activity of the selective ALK inhibitor alectinib in models of intracranial metastases. *Cancer Chemother Pharmacol* **74:**1023-1028.

Kogita A, Togashi Y, Hayashi H, Banno E, Terashima M, De Velasco MA, Sakai K, Fujita Y, Tomida S, Takeyama Y, Okuno K, Nakagawa K, and Nishio K (2015) Activated MET acts as a salvage signal after treatment with alectinib, a selective ALK inhibitor, in ALK-positive non-small cell lung cancer. *Int J Oncol* **46:**1025-1030.

Li J, Jaimes KF, and Aller SG (2014) Refined structures of mouse P-glycoprotein. *Protein Sci* **23:**34-46.

Manolaridis I, Jackson SM, Taylor NMI, Kowal J, Stahlberg H, and Locher KP (2018) Cryo-EM structures of a human ABCG2 mutant trapped in ATP-bound and substrate-bound states. *Nature* **563:**426-430.

Michael M and Doherty MM (2005) Tumoral drug metabolism: overview and its implications for cancer therapy. *J Clin Oncol* **23:**205-229.

Morcos PN, Cleary Y, Guerini E, Dall G, Bogman K, De Petris L, Viteri S, Bordogna W, Yu L, Martin-Facklam M, and Phipps A (2017) Clinical Drug-Drug Interactions Through Cytochrome P450 3A (CYP3A) for the Selective ALK Inhibitor Alectinib. *Clin Pharmacol Drug Dev* **6:**280-291.

Morris GM, Huey R, Lindstrom W, Sanner MF, Belew RK, Goodsell DS, and Olson AJ (2009) AutoDock4 and AutoDockTools4: Automated docking with selective receptor flexibility. *J Comput Chem* **30:**2785-2791.

Muller IB, de Langen AJ, Giovannetti E, and Peters GJ (2017) Anaplastic lymphoma kinase inhibition in metastatic non-small cell lung cancer: clinical impact of alectinib. *Onco Targets Ther* **10:**4535-4541.

Nakagawa T, Fowler S, Takanashi K, Youdim K, Yamauchi T, Kawashima K, Sato-Nakai M, Yu L, and Ishigai M (2018) In vitro metabolism of alectinib, a novel potent ALK inhibitor, in human: contribution of CYP3A enzymes. *Xenobiotica* **48:**546-554.

Prueksaritanont T, Chu X, Gibson C, Cui D, Yee KL, Ballard J, Cabalu T, and Hochman J (2013) Drug-drug interaction studies: regulatory guidance and an industry perspective. *AAPS J* **15:**629-645.

Redaelli S, Ceccon M, Antolini L, Rigolio R, Pirola A, Peronaci M, Gambacorti-Passerini C, and Mologni L (2016) Synergistic activity of ALK and mTOR inhibitors for the treatment of NPM-ALK positive lymphoma. *Oncotarget* **7:**72886-72897.

Robey RW, Pluchino KM, Hall MD, Fojo AT, Bates SE, and Gottesman MM (2018) Revisiting the role of ABC transporters in multidrug-resistant cancer. *Nat Rev Cancer* **18:**452-464.

Rochat B (2009) Importance of influx and efflux systems and xenobiotic metabolizing enzymes in intratumoral disposition of anticancer agents. *Curr Cancer Drug Targets* **9:**652-674.

Siegel RL, Miller KD, and Jemal A (2018) Cancer statistics, 2018. *CA Cancer J Clin* **68:**7-30.

Song Z, Wang M, and Zhang A (2015) Alectinib: a novel second generation anaplastic lymphoma kinase (ALK) inhibitor for overcoming clinically-acquired resistance. *Acta Pharm Sin B* **5:**34-37.

Sorf A, Hofman J, Kucera R, Staud F, and Ceckova M (2018) Ribociclib shows potential for pharmacokinetic drug-drug interactions being a substrate of ABCB1 and potent inhibitor of ABCB1, ABCG2 and CYP450 isoforms in vitro. *Biochem Pharmacol* **154:**10-17.

Szakacs G, Varadi A, Ozvegy-Laczka C, and Sarkadi B (2008) The role of ABC transporters in drug absorption, distribution, metabolism, excretion and toxicity (ADME-Tox). *Drug Discov Today* **13:**379-393.

Trott O and Olson AJ (2010) AutoDock Vina: improving the speed and accuracy of docking with a new scoring function, efficient optimization, and multithreading. *J Comput Chem* **31:**455-461.

UniProt C (2019) UniProt: a worldwide hub of protein knowledge. *Nucleic Acids Res* **47:**D506-D515.

Vadlapatla RK, Vadlapudi AD, Pal D, and Mitra AK (2013) Mechanisms of drug resistance in cancer chemotherapy: coordinated role and regulation of efflux transporters and metabolizing enzymes. *Curr Pharm Des* **19:**7126-7140.

Waterhouse A, Bertoni M, Bienert S, Studer G, Tauriello G, Gumienny R, Heer FT, de Beer TAP, Rempfer C, Bordoli L, Lepore R, and Schwede T (2018) SWISS-MODEL: homology modelling of protein structures and complexes. *Nucleic Acids Res* **46:**W296-W303.

Wienkers LC and Heath TG (2005) Predicting in vivo drug interactions from in vitro drug discovery data. *Nat Rev Drug Discov* **4:**825-833.

Yang K, Chen Y, To KK, Wang F, Li D, Chen L, and Fu L (2017) Alectinib (CH5424802) antagonizes ABCB1- and ABCG2-mediated multidrug resistance in vitro, in vivo and ex vivo. *Exp Mol Med* **49:**e303.

Zhu V and Ou SH (2017) Safety of alectinib for the treatment of metastatic ALK-rearranged non-small cell lung cancer. *Expert Opin Drug Saf* **16:**509-514.

Footnotes

This work was supported by the Czech Science Foundation [grant No. 16-26849S], by the Grant Agency of Charles University [project No. 1568218/C], by the project EFSA-CDN [no. CZ.02.1.01/0.0/0.0/16_019/0000841] co-funded by ERDF, and finally by the Charles University [SVV/2019/260-414, SVV/2019/260-416]. This work was further supported by the European Funds for Regional Development (EFRE) Brandenburg, Germany; project "Entwicklung eines physiologisch relevanten Testsystems zur In-vitro-Erfassung von Hepatotoxizität im Hochdurchsatz" [project No. 85009748]. Computational resources were provided by the CESNET LM2015042 and the CERIT Scientific Cloud LM2015085, provided under the program "Projects of Large Research, Development, and Innovations Infrastructures".

Legends for Figures

Fig. 1. Chemical structure of alectinib.

Fig. 2. Effects of alectinib on intracellular accumulation of Hoechst 33342 or calcein AM in MDCKII-par, MDCKII-ABCB1, MDCKII-ABCG2 and MDCKII-ABCC1 cells. LY335979 (1 μM), Ko143 (1 μM) and MK-571 (25 μM) were used as model inhibitors for the respective transporters. Tested concentrations had been confirmed in our previous studies to yield maximal transporter inhibition. Cells were pre-incubated with alectinib or model inhibitors for 10 min, then 8 μM Hoechst 3342 or 2 μM calcein AM was added and fluorescence was immediately monitored in bottom kinetic mode for 30 min. Data are presented as means ± S.D. obtained from three independent experiments. IC_{50} values were determined as relative ones for which the 100% inhibitory effect was attributed to the alectinib concentration showing the most effective response. Statistical analysis was performed using one-way ANOVA followed by Dunnett's post hoc test (*$p < 0.05$, ***$p < 0.001$ compared to control).

Fig. 3. Effects of alectinib on intracellular accumulation of daunorubicin or mitoxantrone in MDCKII-par, MDCKII-ABCB1, MDCKII-ABCG2 and MDCKII-ABCC1 cells. LY335979 (1 μM), Ko143 (1 μM) and MK-571 (25 μM) were used as model inhibitors for the respective transporters. The tested concentrations had been confirmed in our previous studies to yield maximal transporter inhibition. Cells were pre-incubated with alectinib or model inhibitors for 10 min, then 2 μM daunorubicin or 1 μM mitoxantrone was added. After 1 h incubation, cells were lysed and fluorescence was detected in lysates. Data are expressed as means ± S.D. obtained from three independent experiments. IC_{50} values were determined as relative ones for which the 100% inhibitory effect was attributed to the alectinib concentration showing the

most effective response. Statistical analysis was performed using one-way ANOVA followed by Dunnett's post hoc test (*$p < 0.05$, **$p < 0.01$, ***$p < 0.001$ compared to control).

Fig. 4. Molecular docking of alectinib into ABCB1 and ABCG2 structures. (A) Rigid molecular docking of alectinib into the inward-facing form of ABCB1. Eight top-ranked positions of alectinib (-10.2 to -8.7 kcal/mol) (magenta) in the protein backbone (green image) are shown. (B) Flexible molecular docking of alectinib into M- and R-sites of ABCB1. The pose with the lowest minimal binding energy is shown for the M-site (-12.5 kcal/mol) and R-site (-9.4 kcal/mol). Alectinib is depicted in magenta; protein residues surrounding the ligand within 4.5 Å are shown as green sticks and labeled. (C) Flexible molecular docking of alectinib into NBDs of ABCB1. The pose with the lowest binding energy is shown for each ATP binding site (-12.3 and -12.1 kcal/mol). Alectinib is shown in magenta, ATP originally co-crystallized in protein backbone as cyan sticks. (D) Orientation of alectinib in ABCG2 as determined by flexible docking analysis. Alectinib molecules are depicted in magenta (-13.1 and -13.0 kcal/mol). Cholesterol, which is known to have an essential role for ABCG2 function, is shown as yellow sticks. (E) Orientation of alectinib in NBDs of ABCG2 predicted by rigid docking analysis. Alectinib (magenta) may compete with ATP (cyan) for binding (-8.8 and -8.6 kcal/mol) to NBDs.

Fig. 5. Effect of alectinib on antiproliferative activities of daunorubicin and mitoxantrone in MDCKII and A431 cells. The cells were exposed to the tested cytostatic drugs or their combinations with 2 μM (daunorubicin combinations) or 1 μM alectinib (mitoxantrone combinations), and cell viability was determined after 48 h of incubation using MTT proliferation test. The data obtained are further analyzed in Table 1 and Fig. 6. Values are presented as means ± S.D. from three independent experiments.

Fig. 6. Combination index analysis of the effects of 2 or 1 μM alectinib on antiproliferative activities of daunorubicin or mitoxantrone, respectively, in MDCKII and A431 cells. Values shown in Fig. 5 together with alectinib proliferation data (not shown) were analyzed using CompuSyn software obtaining CI plots. (A) alectinib + daunorubicin combination in MDCKII-ABCB1 cells, (B) alectinib + mitoxantrone combination in MDCKII-ABCG2 cells, (C) alectinib + daunorubicin combination in MDCKII-ABCB1 cells, and (D) alectinib + mitoxantrone combination in MDCKII-ABCG2 cells According to the median-effect analysis principle developed by Chou-Talalay, CI < 0.9 determines synergistic effect of drug combination, CI > 0.9 and < 1.1 additive effect, and CI > 1.1 antagonistic effect. The data points are presented as means ± S.D. coming from three independent experiments.

Fig. 7. Effects of ABCB1, ABCG2 and ABCC1 on cellular response to alectinib. The cells were exposed to alectinib and cell viabilities were determined after 48 h of incubation using MTT proliferation test. Due to limited solubility of alectinib, concentrations higher than 7.5 μM could not be tested. Data were analyzed statistically using one-way ANOVA followed by Dunnett's post hoc test. ABC transporter-overexpressing cell viability values from each particular concentration point were compared to the corresponding viability values from parent cells, but no statistically significant changes were recorded for any of the points. Data are expressed as means ± S.D. from three independent experiments.

Fig. 8. Inhibitory effects of alectinib toward human CYP1A2, CYP3A4, CYP3A5, CYP2B6, CYP2C19, CYP2C8, CYP2C9 and CYP2D6 assessed employing commercial Vivid CYP450 Screening Kits. Evaluation of data was performed after 15 min incubation interval. The enzyme concentrations were within the linear part of the appropriate reaction velocity curves at this interval. To normalize data, fluorescence of samples where only enzyme and 0.5%

DMSO instead of the tested drug were present was considered as maximal (100%) enzyme activity. Fluorescence equal to 0% activity was obtained from the samples incubated with enzyme solvent buffer without enzyme and 0.5% DMSO. Alectinib concentrations were adjusted by pre-dilution in DMSO so that 0.5% DMSO was introduced into reaction mixtures at all concentration points. Data are expressed as means ± S.D. from three independent experiments.

Fig. 9. Effects of 0.5 μM alectinib on mRNA levels of *ABCB1*, *ABCG2* and *ABCC1* in (B, C) intestine and (D, E) NSCLC cellular models. *CYP1A2*, *CYP3A4* and *CYP2B6* genes were evaluated in (F) proliferation-competent primary-like human hepatocytes HepaFH3. Alectinib concentration of 0.5 μM was selected based on (A) the results of proliferation MTT tests that were performed prior to induction studies and C_{max} of alectinib. In induction experiments, cells were incubated with 0.5 μM alectinib and mRNA of target genes was quantified at 24 and 48 h intervals using qRT-PCR. Relative quantification of the examined ABC transporters and CYP enzymes was performed using the ΔΔCt method, with the geometric means of *B2M* and *HPRT1* levels used as internal controls to normalize the variability in expression levels. Data are expressed as means ± S.D. from three experiments.

DMD Fast Forward. Published on May 8, 2019 as DOI: 10.1124/dmd.119.086975
This article has not been copyedited and formatted. The final version may differ from this version.

Tables

Table 1. Analysis of the effect of simultaneous administration of alectinib with model cytotoxic drugs in MDCKII and A431 cells

Cell line	Drug(s)[a]	IC_{50}[b] (μM)	95% CI (μM)	Fold reversal[c]	Normalized fold reversal[d]
MDCKII-parent					
	daunorubicin	0.993	(0.867-1.13)		
	mitoxantrone	1.60	(1.43-1.81)		
	daunorubicin + alectinib	0.345*	(0.295-0.400)	2.88	
	mitoxantrone + alectinib	1.13ns	(0.909-1.40)	1.42	
MDCKII-ABCB1					
	daunorubicin	12.1	(11.6-12.7)		
	daunorubicin + alectinib	0.681*	(0.650-0.714)	17.8	6.18
MDCKII-ABCG2					
	mitoxantrone	9.55	(9.00-10.1)		
	mitoxantrone + alectinib	0.991**	(0.707-1.29)	9.64	6.79
A431-parent					
	daunorubicin	0.378	(0.204-0.749)		
	mitoxantrone	0.290	(0.165-0.501)		
	daunorubicin + alectinib	0.0333ns	(0.0211-0.0514)	11.4	
	mitoxantrone + alectinib	0.0315ns	(0.0152-0.0582)	9.21	
A431-ABCB1					
	daunorubicin	5.95	(4.54-7.73)		
	daunorubicin + alectinib	0.244***	(0.126-0.334)	24.4	2.14

A431-ABCG2

mitoxantrone	6.91	(5.56-8.52)		
mitoxantrone + alectinib	0.156**	(0.111-0.220)	44.3	4.81

[a] Alectinib in concentration of 2 or 1 μM was used in daunorubicin and mitoxantrone combinations, respectively.

[b] Values were calculated from the data shown in Fig. 5. IC_{50} values from drug combinations were compared with IC_{50} values from single drug treatments in particular cell lines using two-tailed unpaired *t*-tests (*$p < 0.05$, **$p < 0.01$, ***$p < 0.001$).

[c] Fold reversal values were calculated as the ratio of IC_{50} from single drug treatment to IC_{50} of combined drug treatment in the particular cell line.

[d] Normalized fold reversal data represent the ratio of IC_{50} from combined drug treatment in transporter-overexpressing cells to IC_{50} from combined drug treatment in corresponding parent cells.

DMD Fast Forward. Published on May 8, 2019 as DOI: 10.1124/dmd.119.086975
This article has not been copyedited and formatted. The final version may differ from this version.

Figures

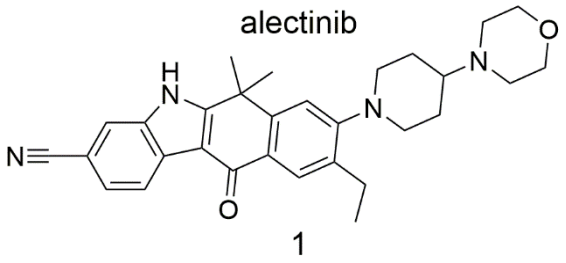

1

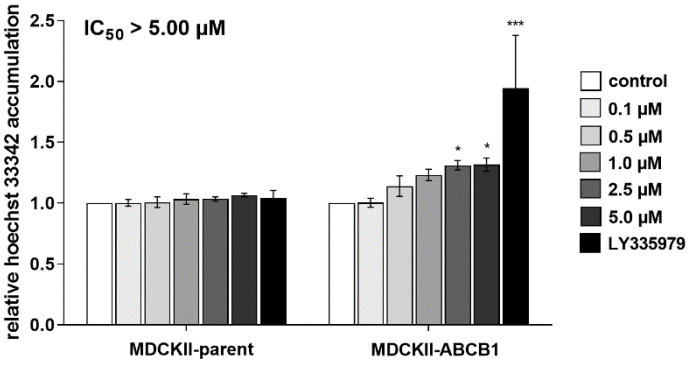

2

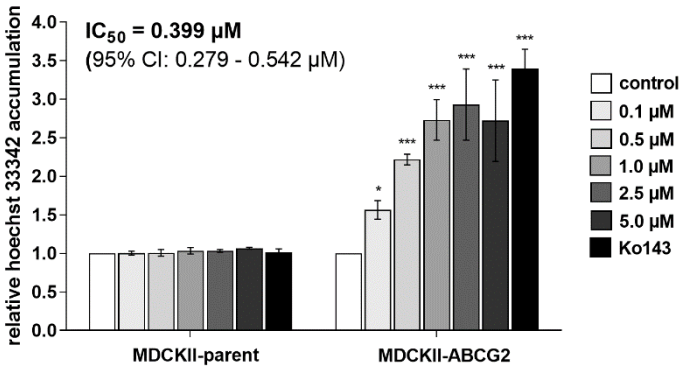

2

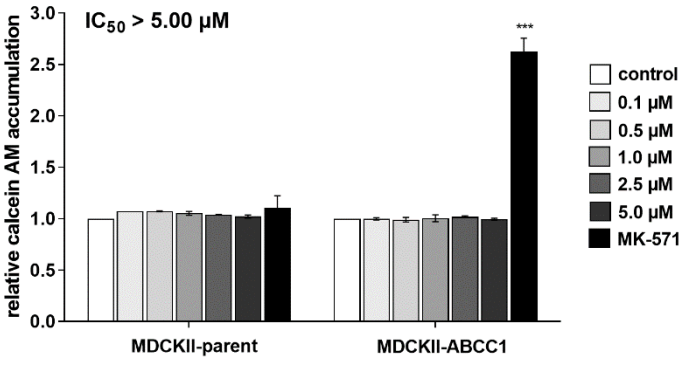

2

DMD Fast Forward. Published on May 8, 2019 as DOI: 10.1124/dmd.119.086975
This article has not been copyedited and formatted. The final version may differ from this version.

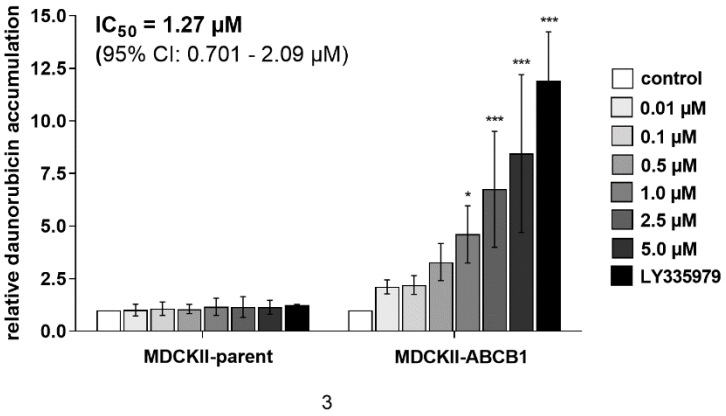

3

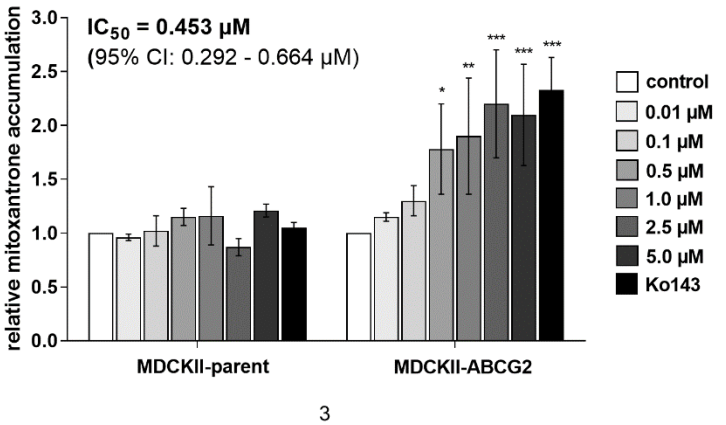

3

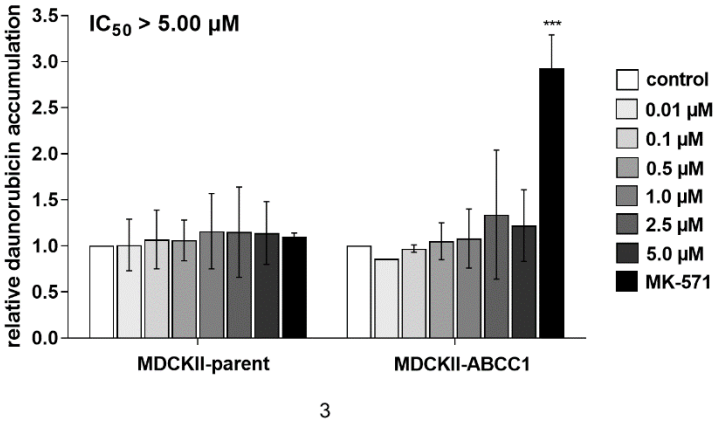

3

DMD Fast Forward. Published on May 8, 2019 as DOI: 10.1124/dmd.119.086975
This article has not been copyedited and formatted. The final version may differ from this version.

A

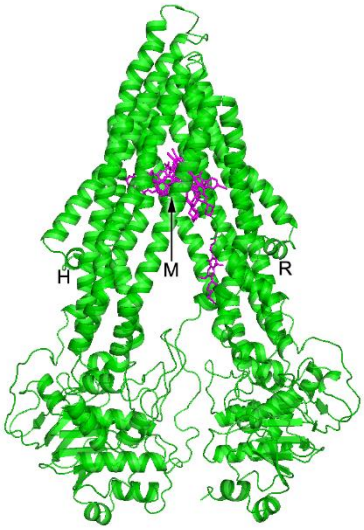

4

B

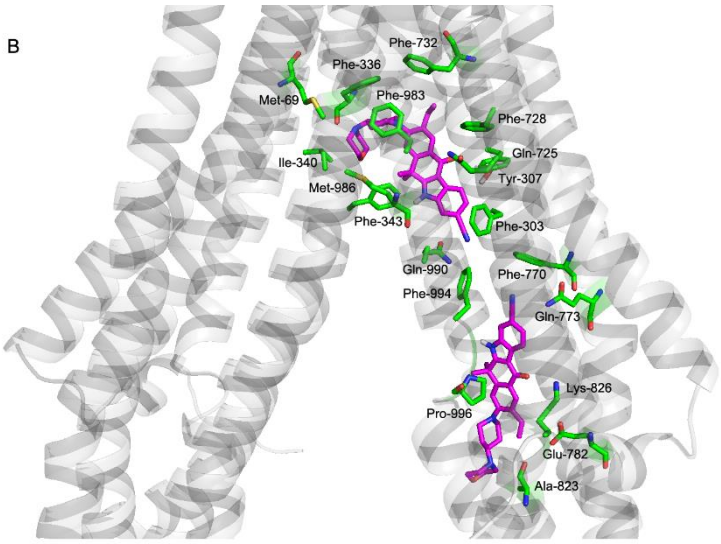

4

C

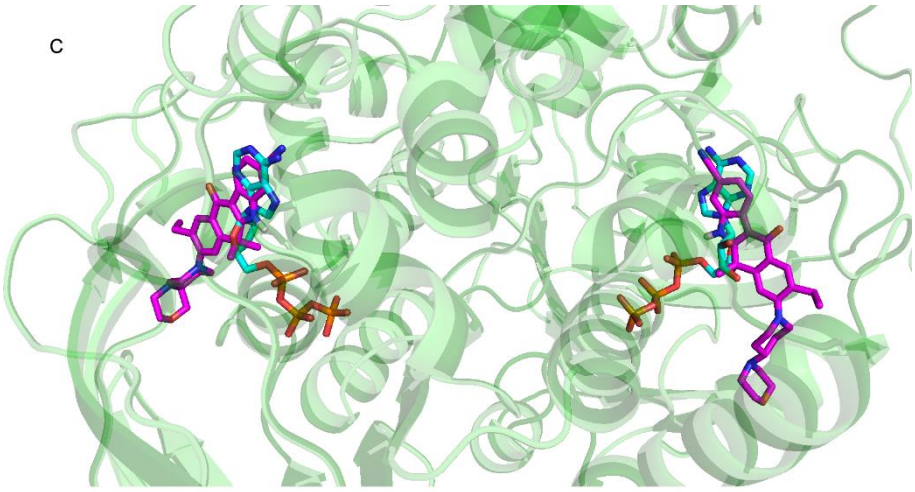

4

DMD Fast Forward. Published on May 8, 2019 as DOI: 10.1124/dmd.119.086975
This article has not been copyedited and formatted. The final version may differ from this version.

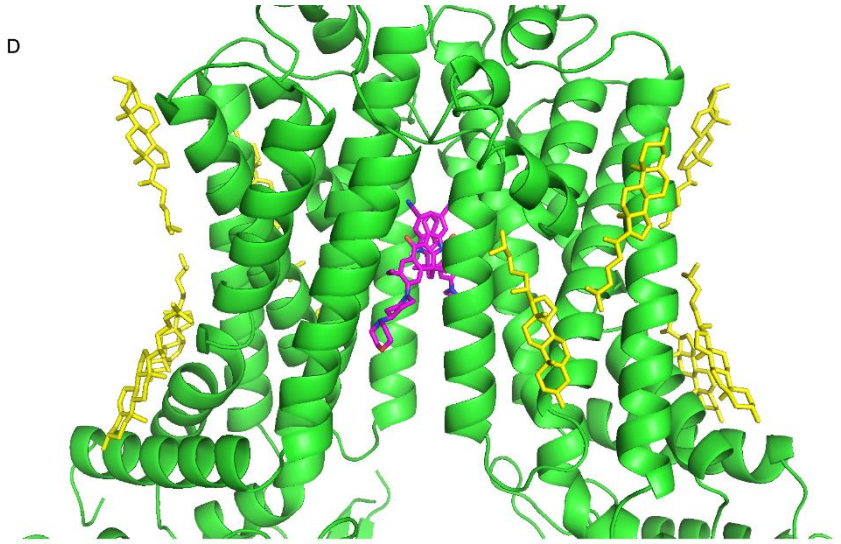

4

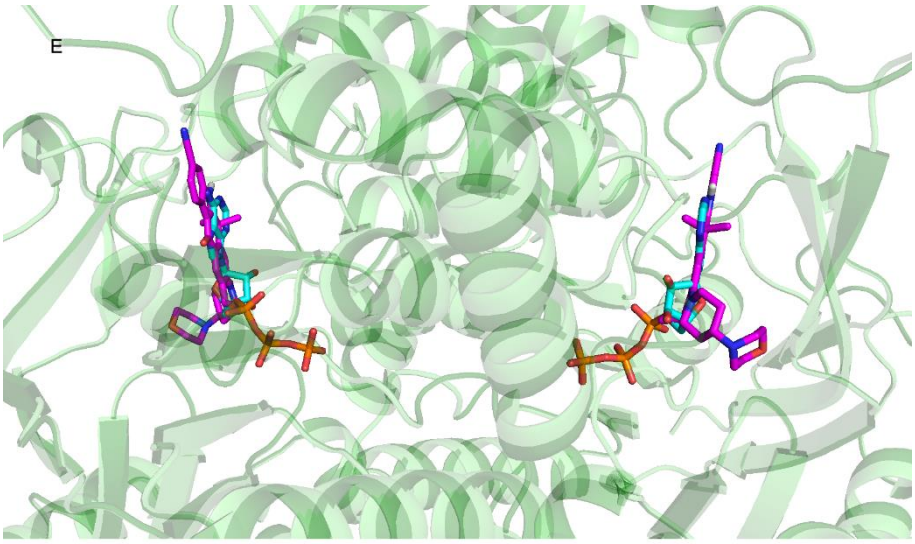

4

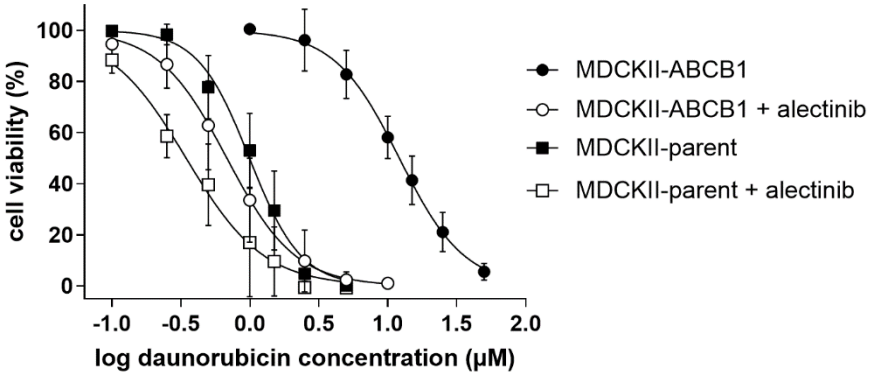

5

DMD Fast Forward. Published on May 8, 2019 as DOI: 10.1124/dmd.119.086975
This article has not been copyedited and formatted. The final version may differ from this version.

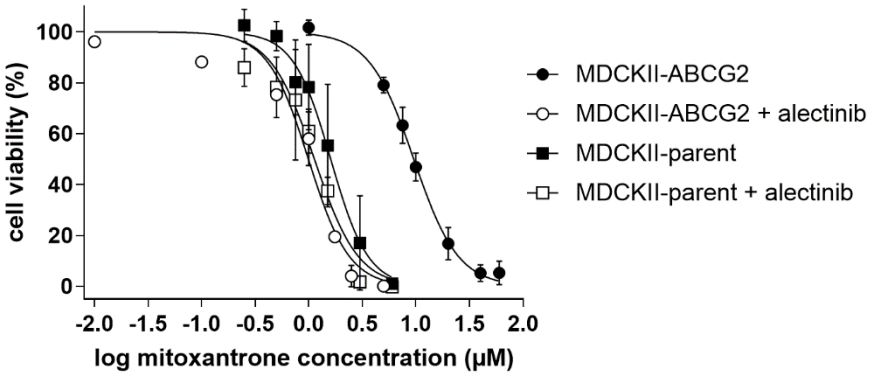

5

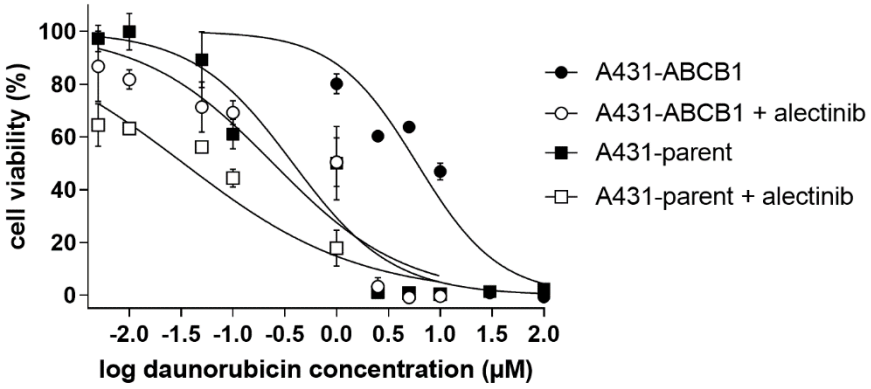

5

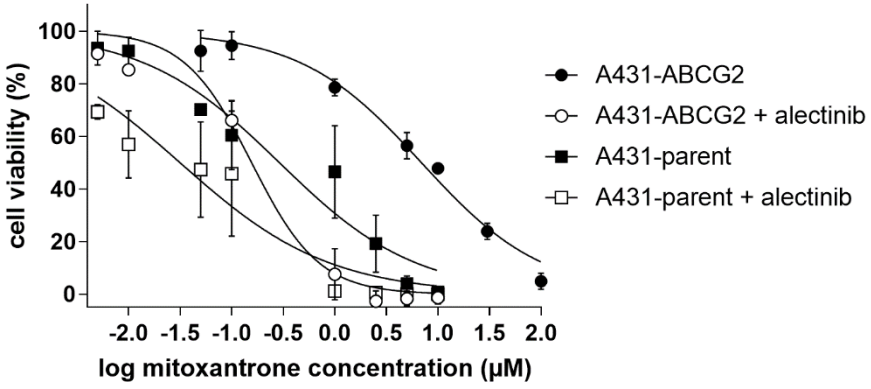

5

DMD Fast Forward. Published on May 8, 2019 as DOI: 10.1124/dmd.119.086975
This article has not been copyedited and formatted. The final version may differ from this version.

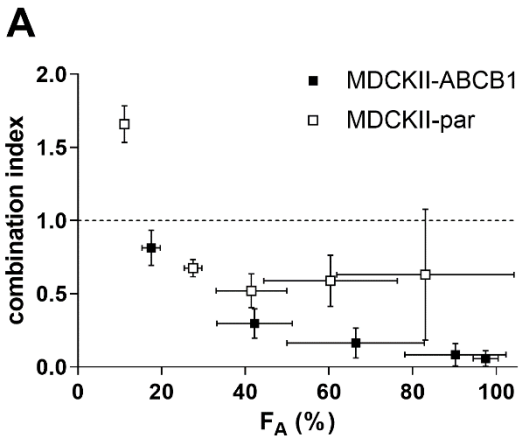

6

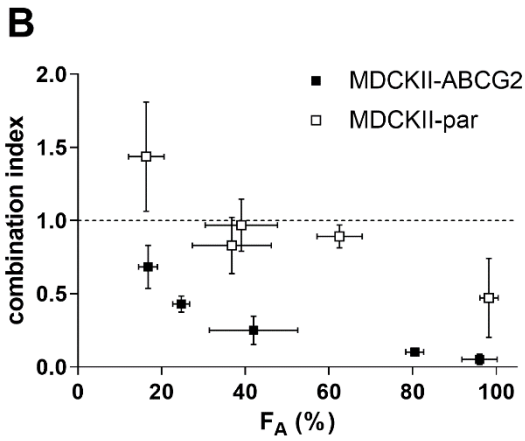

6

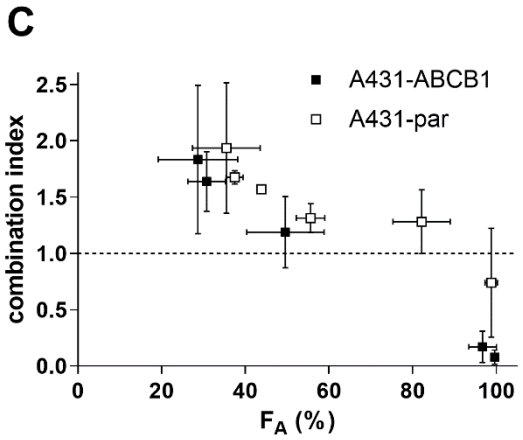

6

DMD Fast Forward. Published on May 8, 2019 as DOI: 10.1124/dmd.119.086975
This article has not been copyedited and formatted. The final version may differ from this version.

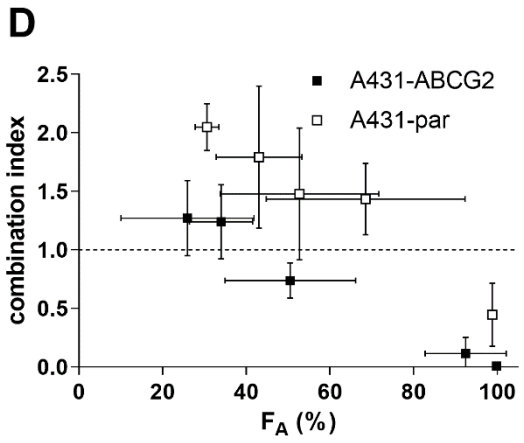

6

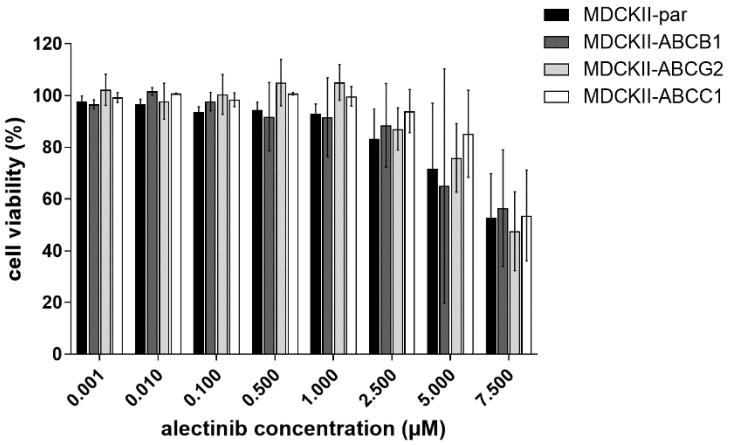

7

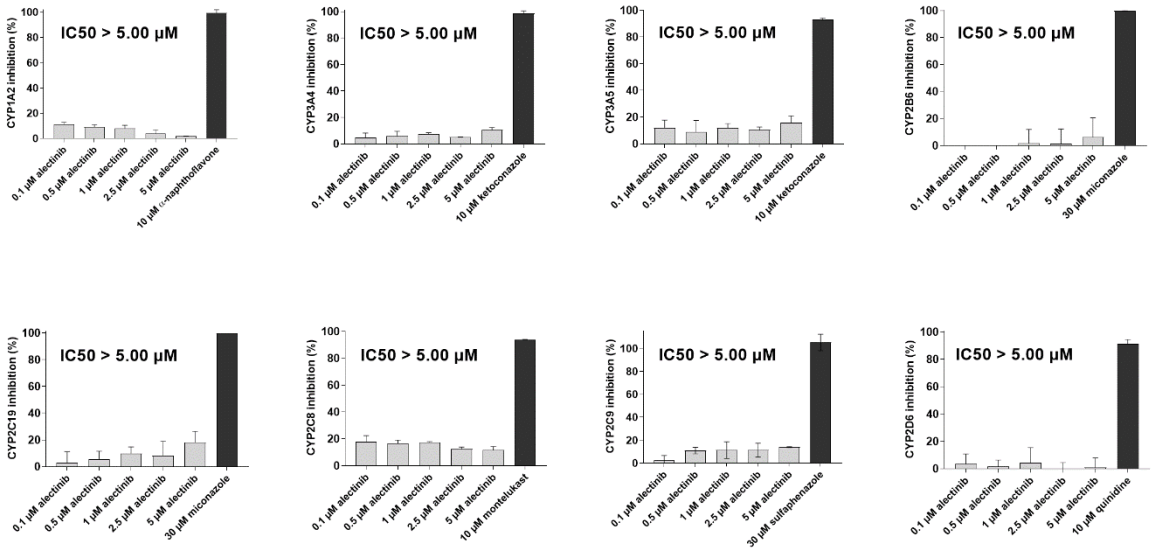

8

DMD Fast Forward. Published on May 8, 2019 as DOI: 10.1124/dmd.119.086975
This article has not been copyedited and formatted. The final version may differ from this version.

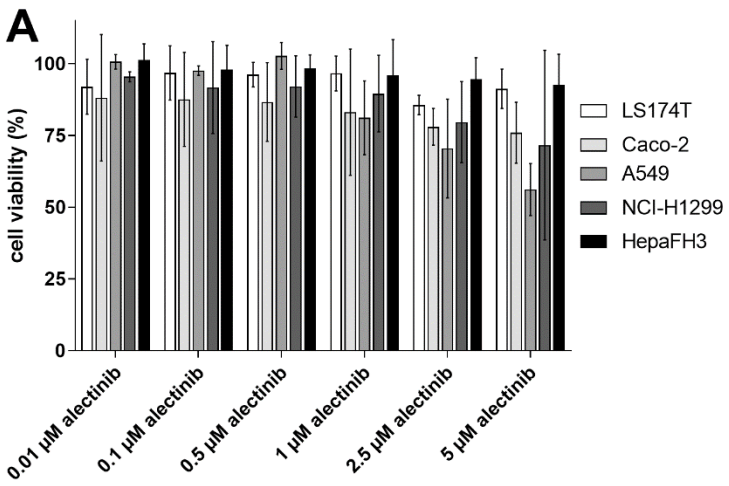

9

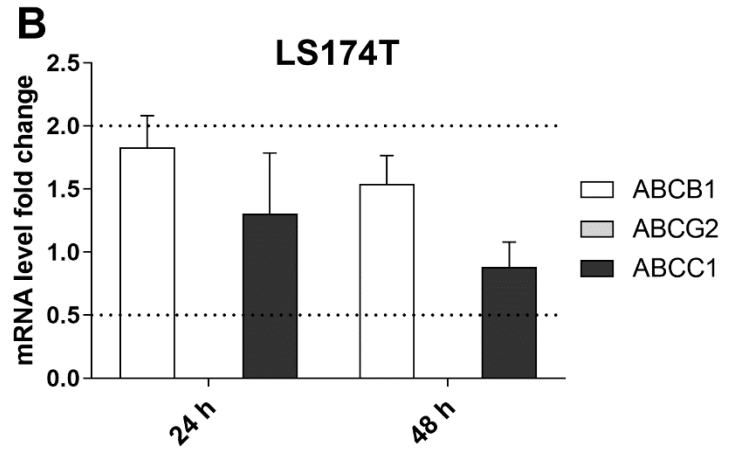

9

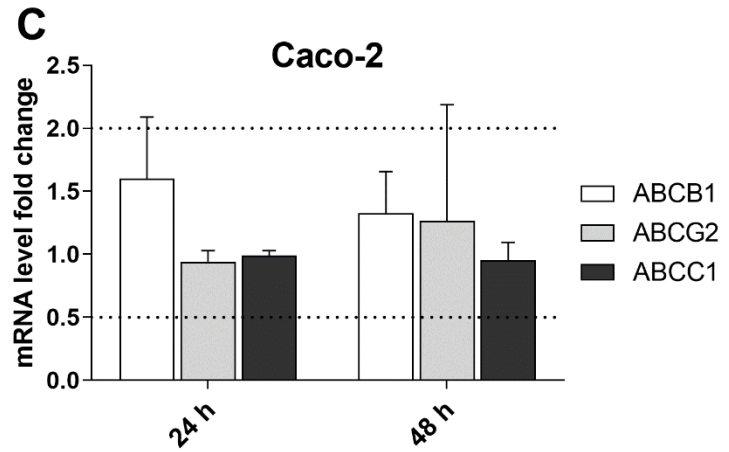

9

DMD Fast Forward. Published on May 8, 2019 as DOI: 10.1124/dmd.119.086975
This article has not been copyedited and formatted. The final version may differ from this version.

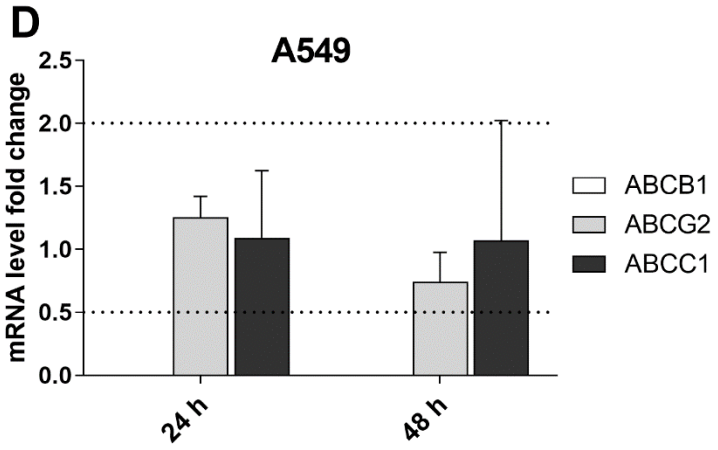

9

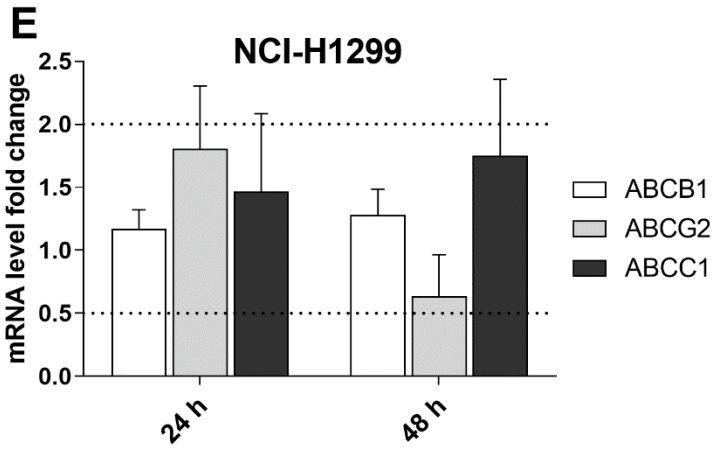

9

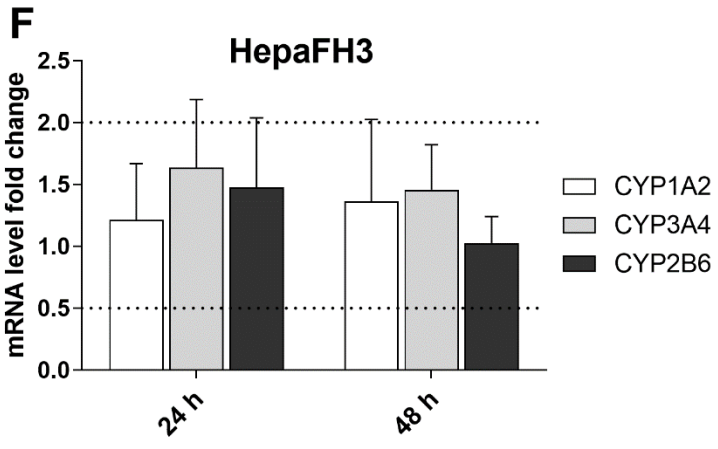

9